Pseudogapped Mott criticality: Stretching Kondo Screening to Breaking Point

How a Fermi liquid gives way to Mott insulator in 2D

Abhirup Mukherjee, Siddhartha Lal

Department of Physical Sciences,
Indian Institute of Science Education and Research Kolkata

May 7, 2025

Some Questions

The anomalous **pseudogap** (PG) phase exhibits nodal-antinodal dichotomy.

No general consensus yet regarding

- nature of $T = 0$ ground states of the cuprates
- **relation** of PG to Mott insulating and superconducting phases proximate to it
- how pseudogap **evolves** from weak- to strong-coupling
- nature of correlations and entanglement within the transition to the model

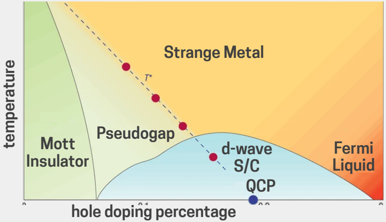

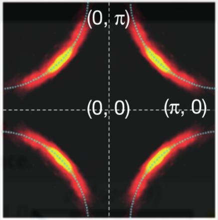

Keimer et al. 2015; Proust and Taillefer 2019; Loeser et al. 1996; Norman et al. 1998; Hashimoto et al. 2014; Kyung et al. 2006; Macridin et al. 2006; Wu et al. 2018; Mukherjee and Lal 2020; Hille et al. 2020.

New Auxiliary Model Approach To Interacting Fermions

1. Solve an appropriate **impurity model**, H_{imp}
   - Lattice symmetry
   - Impurity phase transition

2. **Construct lattice** model by applying many-body translation operators:

$$H_{\text{latt}} = \sum_{\mathbf{r}} T^{\dagger}(\mathbf{r}) H_{\text{imp}}(\mathbf{r_0}) T(\mathbf{r})$$

3. Relate computables across the models, using many-body Bloch's theorem

Greens functions:

$$\tilde{G}(\mathbf{K}\sigma; \omega) = G^{>}(T^{\dagger}_{\mathbf{K}\sigma}, \omega - \varepsilon_{\mathbf{K}}) + G^{<}(T^{\dagger}_{\mathbf{K}\sigma}, \omega + \varepsilon_{\mathbf{K}})$$

Equal-time **correlation** functions:

$$C_O(\mathbf{k}_1, \mathbf{k}_2) = \sum_{\Delta} \langle \mathbf{r}_c + \Delta | \tilde{O}(\mathbf{k}_2) | \mathbf{r}_c \rangle \langle \mathbf{r}_c | \tilde{O}^{\dagger}(\mathbf{k}_1) | \mathbf{r}_c \rangle$$

where

$$G^{>}(O^{\dagger}, t) = -i \langle O(t) O^{\dagger} \rangle,$$

(imp-bath T-matrix)

$$T_{\mathbf{K}\sigma} = c_{\mathbf{K}\sigma} \left(\textstyle\sum_{\sigma'} c^{\dagger}_{d\sigma} + \text{h.c.} \right) + c_{\mathbf{K}\sigma} \left(S^{+}_{d} + \text{h.c.} \right),$$

$$\tilde{O}(\mathbf{r}) = O(\mathbf{r}) O^{\dagger}(d)$$

Stoyanova 2006; Maier et al. 2005; Sakai 2023.

The Core Ingredient: A Lattice-Embedded Impurity Model

$$H_{\text{imp}} = H_{\text{2D-TB-KE}} + V \sum_{Z,\sigma} \left(c^{\dagger}_{d\sigma} c_{Z\sigma} + \text{h.c.}\right) + J \sum_{Z} \mathbf{S}_d \cdot \mathbf{S}_Z - \frac{W}{2} \sum_{Z} \left(n_{Z\uparrow} - n_{Z\downarrow}\right)^2$$

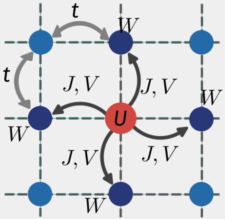

- $J_{\mathbf{k},\mathbf{k}'}$ has C_4**-symmetry** instead of s-wave symmetry

$$J_{\mathbf{k},\mathbf{k}'} = \frac{J}{2}\left[\cos\left(\mathbf{k}_x - \mathbf{k}'_x\right) + \cos\left(\mathbf{k}_y - \mathbf{k}'_y\right)\right]$$

Kai-Hua et al. 2002.

The Core Ingredient: A Lattice-Embedded Impurity Model

$$H_{\mathrm{imp}} = H_{\text{2D-TB-KE}} + V\sum_{Z,\sigma}\left(c^\dagger_{d\sigma}c_{Z\sigma} + \text{h.c.}\right) + J\sum_{Z}\mathbf{S}_d\cdot\mathbf{S}_Z - \frac{W}{2}\sum_{Z}\left(n_{Z\uparrow} - n_{Z\downarrow}\right)^2$$

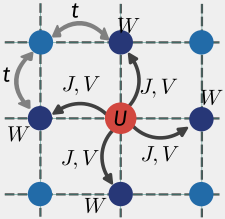

- $J_{\mathbf{k},\mathbf{k}'}$ has C_4**–symmetry** instead of s–wave symmetry

$$J_{\mathbf{k},\mathbf{k}'} = \frac{J}{2}\left[\cos\left(\mathbf{k}_x - \mathbf{k}'_x\right) + \cos\left(\mathbf{k}_y - \mathbf{k}'_y\right)\right]$$

Map to Hubbard-Heisenberg Model

$$H_{\mathrm{latt}} = \sum_{\mathbf{r}} T^\dagger(\mathbf{r})H_{\mathrm{imp}}(\mathbf{r_0})T(\mathbf{r})$$

$$= -\frac{\tilde{t}}{\sqrt{Z}}\sum_{\langle \mathbf{r}_i,\mathbf{r}_j\rangle;\sigma}\left(c^\dagger_{\mathbf{r}_i,\sigma}c_{\mathbf{r}_j,\sigma} + \text{h.c.}\right) - \tilde{\mu}\sum_{\mathbf{r}}\hat{n}_{\mathbf{r},\sigma}$$

$$+ \frac{\tilde{J}}{Z}\sum_{\langle \mathbf{r}_i,\mathbf{r}_j\rangle}\mathbf{S}_{\mathbf{r}_i}\cdot\mathbf{S}_{\mathbf{r}_j} - \frac{1}{2}\tilde{U}\sum_{\mathbf{r}}\left(\hat{n}_{\mathbf{r},\uparrow} - \hat{n}_{\mathbf{r},\downarrow}\right)^2$$

$$\tilde{t} = t + 2V$$

$$\tilde{U} = U + W$$

$$\tilde{\mu} = 2\mu + \eta, \quad \tilde{J} = 2J$$

Kai-Hua et al. 2002.

The Core Ingredient: A Lattice-Embedded Impurity Model

$$H_{\text{imp}} = H_{\text{2D-TB-KE}} + V\sum_{Z,\sigma}\left(c^{\dagger}_{d\sigma}c_{Z\sigma} + \text{h.c.}\right) + J\sum_{Z}\mathbf{S}_d\cdot\mathbf{S}_Z - \frac{W}{2}\sum_{Z}\left(n_{Z\uparrow} - n_{Z\downarrow}\right)^2$$

- $J_{\mathbf{k},\mathbf{k}'}$ has C_4**-symmetry** instead of s-wave symmetry

$$J_{\mathbf{k},\mathbf{k}'} = \frac{J}{2}\left[\cos\left(\mathbf{k}_x - \mathbf{k}'_x\right) + \cos\left(\mathbf{k}_y - \mathbf{k}'_y\right)\right]$$

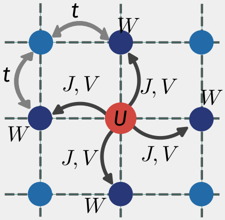

Map to Hubbard-Heisenberg Model

$$H_{\text{latt}} = \sum_{\mathbf{r}} T^{\dagger}(\mathbf{r})H_{\text{imp}}(\mathbf{r_0})T(\mathbf{r})$$

$$= -\frac{\tilde{t}}{\sqrt{Z}}\sum_{\langle\mathbf{r}_i,\mathbf{r}_j\rangle;\sigma}\left(c^{\dagger}_{\mathbf{r}_i,\sigma}c_{\mathbf{r}_j,\sigma} + \text{h.c.}\right) - \tilde{\mu}\sum_{\mathbf{r}}\hat{n}_{\mathbf{r},\sigma}$$

$$+\frac{\tilde{J}}{Z}\sum_{\langle\mathbf{r}_i,\mathbf{r}_j\rangle}\mathbf{S}_{\mathbf{r}_i}\cdot\mathbf{S}_{\mathbf{r}_j} - \frac{1}{2}\tilde{U}\sum_{\mathbf{r}}\left(\hat{n}_{\mathbf{r},\uparrow} - \hat{n}_{\mathbf{r},\downarrow}\right)^2$$

$$\tilde{t} = t + 2V$$

$$\tilde{U} = U + W$$

$$\tilde{\mu} = 2\mu + \eta, \quad \tilde{J} = 2J$$

- We work in large U limit
- SW transformation $\rightarrow$ $J - W$ **model**

Kai-Hua et al. 2002.

Pseudogapping Transition from Kondo Breakdown

Unitary RG analysis - integrate out high-energy states in the conduction bath:

$$\Delta J^{(j)}_{\mathbf{k}_1,\mathbf{k}_2} = -\sum_{\mathbf{q}\in \mathrm{PS}} \frac{J^{(j)}_{\mathbf{k}_2,\mathbf{q}} J^{(j)}_{\mathbf{q},\mathbf{k}_1} + 4J^{(j)}_{\mathbf{q},\bar{\mathbf{q}}} W_{\bar{\mathbf{q}},\mathbf{k}_2,\mathbf{k}_1,\mathbf{q}}}{\omega - \frac{1}{2}|\varepsilon_j| + J^{(j)}_{\mathbf{q}}/4 + W_{\mathbf{q}}/2}$$

Pseudogapping Transition from Kondo Breakdown

Unitary RG analysis - integrate out high-energy states in the conduction bath:

$$\Delta J^{(j)}_{\mathbf{k}_1,\mathbf{k}_2} = -\sum_{\mathbf{q}\in \mathrm{PS}} \frac{J^{(j)}_{\mathbf{k}_2,\mathbf{q}} J^{(j)}_{\mathbf{q},\mathbf{k}_1} + 4J^{(j)}_{\mathbf{q},\bar{\mathbf{q}}} W_{\bar{\mathbf{q}},\mathbf{k}_2,\mathbf{k}_1,\mathbf{q}}}{\omega - \frac{1}{2}|\varepsilon_j| + J^{(j)}_{\mathbf{q}}/4 + W_{\mathbf{q}}/2}$$

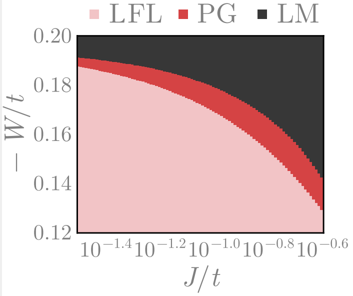

- momentum-**anistropic** screened phase between SC and LM phases.
- Contrast with **eSIAM**: $\Delta J \sim J(J + 4W)$

Pseudogapping Transition from Kondo Breakdown

Unitary RG analysis - integrate out high-energy states in the conduction bath:

$$\Delta J^{(j)}_{\mathbf{k}_1,\mathbf{k}_2} = -\sum_{\mathbf{q}\in \mathrm{PS}} \frac{J^{(j)}_{\mathbf{k}_2,\mathbf{q}} J^{(j)}_{\mathbf{q},\mathbf{k}_1} + 4 J^{(j)}_{\mathbf{q},\bar{\mathbf{q}}} W_{\bar{\mathbf{q}},\mathbf{k}_2,\mathbf{k}_1,\mathbf{q}}}{\omega - \frac{1}{2}|\varepsilon_j| + J^{(j)}_{\mathbf{q}}/4 + W_{\mathbf{q}}/2}$$

- momentum-**anistropic** screened phase between SC and LM phases.
- Contrast with **eSIAM**: $\Delta J \sim J(J + 4W)$
- Impurity-bath spin correlations show k-differentiation

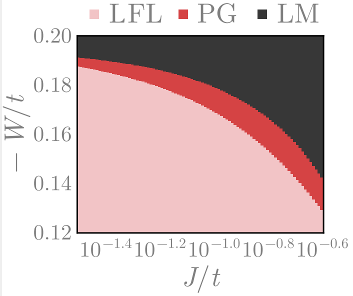

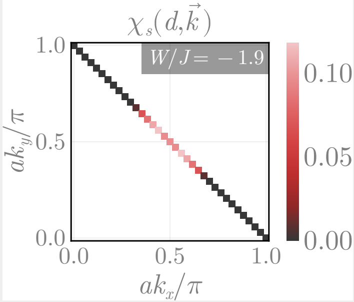

Pseudogapping Transition from Kondo Breakdown

Unitary RG analysis - integrate out high-energy states in the conduction bath:

$$\Delta J^{(j)}_{\mathbf{k}_1,\mathbf{k}_2} = -\sum_{\mathbf{q}\in \mathrm{PS}} \frac{J^{(j)}_{\mathbf{k}_2,\mathbf{q}} J^{(j)}_{\mathbf{q},\mathbf{k}_1} + 4 J^{(j)}_{\mathbf{q},\bar{\mathbf{q}}} W_{\bar{\mathbf{q}},\mathbf{k}_2,\mathbf{k}_1,\mathbf{q}}}{\omega - \frac{1}{2}|\varepsilon_j| + J^{(j)}_{\mathbf{q}}/4 + W_{\mathbf{q}}/2}$$

- momentum-**anistropic** screened phase between SC and LM phases.
- Contrast with **eSIAM**: $\Delta J \sim J(J + 4W)$
- Impurity-bath spin correlations show k-differentiation
- Lattice model DOS shows **P-gap**

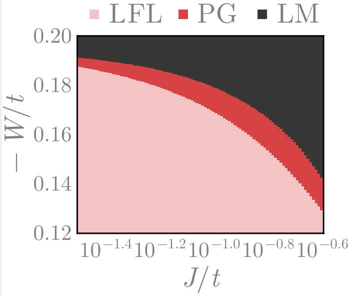

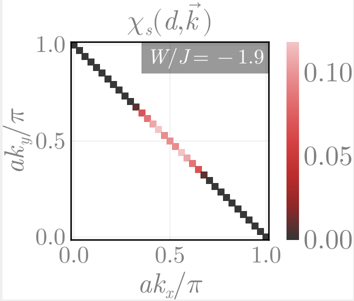

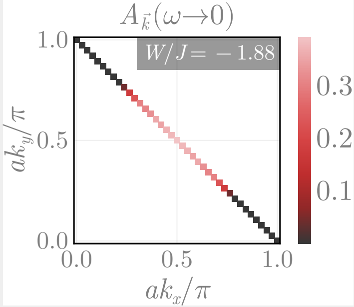

Local Fermi Liquid and Local Moment Phases

LFL

- Democratic screening in k-space, broad $\omega = 0$ **resonance**
- 1-particle excitations → Fermi liquid upon tiling
- $\Sigma'' \sim \omega^2$

These phases also exist in the **eSIAM**.

LM

- Unscreened moment. Spectral function gapped.
- $\Sigma \sim 1/\omega$
- Irrelevant hopping processes lead to Heisenberg model

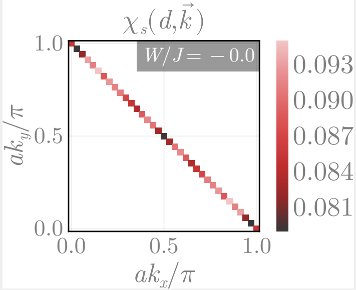

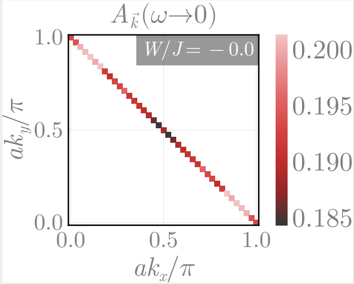

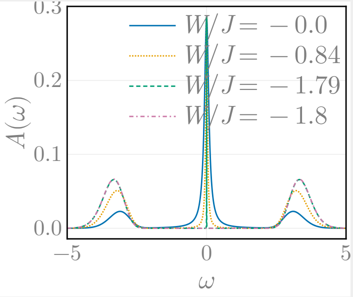

Unravelling of Kondo screening

The Kondo breakdown process can be visualised in terms of **zeros** of $J_{\mathbf{k}_N,\mathbf{k}}$.

- $J_{\mathbf{k}_N,\mathbf{k}}$ for $\mathbf{k}$ close to the **adjacent nodes** turn RG irrelevant first, and a patch of zeros subsequently appears in $J_{\mathbf{k}_N,\mathbf{k}}$ around this point.

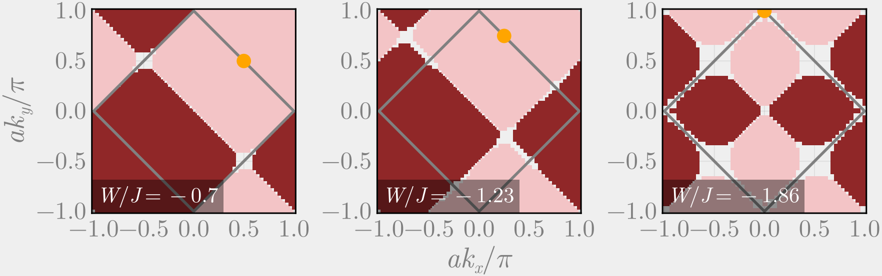

Unravelling of Kondo screening

The Kondo breakdown process can be visualised in terms of **zeros** of $J_{\mathbf{k}_N,\mathbf{k}}$.

- $J_{\mathbf{k}_N,\mathbf{k}}$ for $\mathbf{k}$ close to the **adjacent nodes** turn RG irrelevant first, and a patch of zeros subsequently appears in $J_{\mathbf{k}_N,\mathbf{k}}$ around this point.
- Tuning W/J further extends the patch of zeros in $J_{\mathbf{k}_1,\mathbf{k}_2}$ for all $\mathbf{k}_1$ lying between a given node and the nearest antinodes.

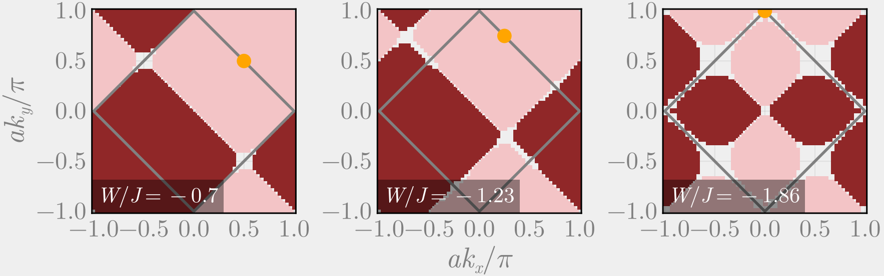

Unravelling of Kondo screening

The Kondo breakdown process can be visualised in terms of **zeros** of $J_{\mathbf{k}_N,\mathbf{k}}$.

- $J_{\mathbf{k}_N,\mathbf{k}}$ for $\mathbf{k}$ close to the **adjacent nodes** turn RG irrelevant first, and a patch of zeros subsequently appears in $J_{\mathbf{k}_N,\mathbf{k}}$ around this point.
- Tuning W/J further extends the patch of zeros in $J_{\mathbf{k}_1,\mathbf{k}_2}$ for all $\mathbf{k}_1$ lying between a given node and the nearest antinodes.
- At $W = W_{\text{PG}}$, the **antinode** joins this connected region of zeros in $J_{\mathbf{k}_1,\mathbf{k}_2}$, marking the onset of the PG. The antinode **decouples** from all Fermi points.

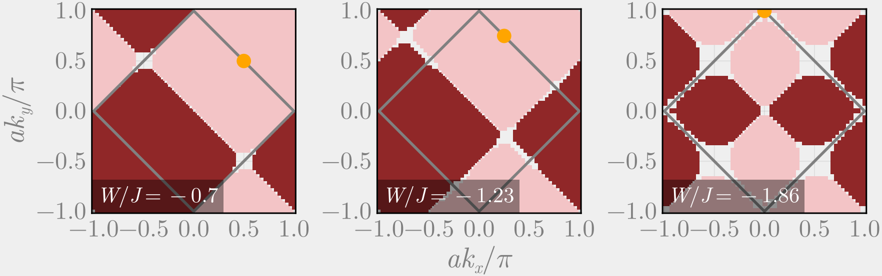

Dynamical Spectral Weight Transfer

- strong fluctuations observed in **charge correlations** between the gapless nodal and gapped antinodal regions in PG regime
- PG results from **selective transfer** of spectral weight from low to high energies
- **Differs from eSIAM** (spectral weight transferred from entire FS at once)
- PG coincides with the appearance of poles of the lattice self-energy $\Sigma(\mathbf{k}, \omega = 0)$ near the antinodes

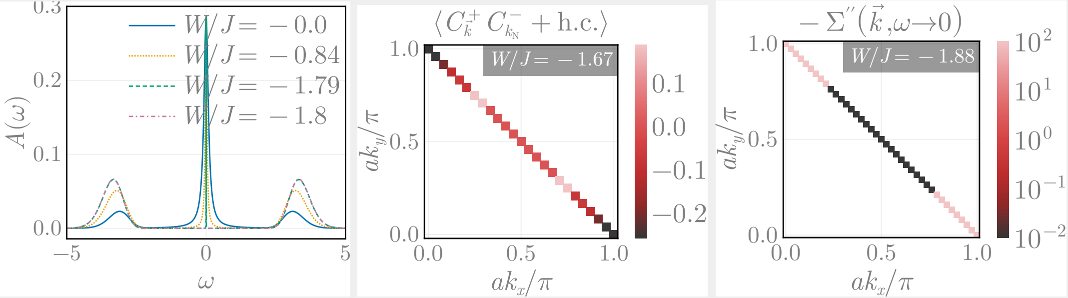

Non-Fermi liquid nature of the pseudogap

Kondo scattering processes can be divided into two classes

- $H_{\mathrm{ch1}}, H_{\mathrm{ch2}}$: **Within** the green/pink regions
- H_{1-2}: **Connecting** the green and pink regions
- Fermi liquid: $H_{\mathrm{ch1}} = H_{\mathrm{ch2}} \simeq H_{1-2}$

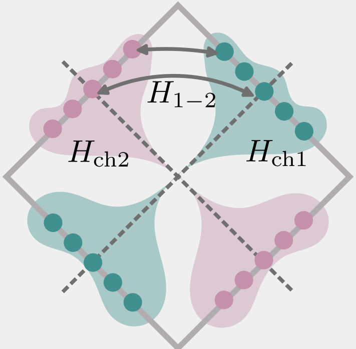

Non-Fermi liquid nature of the pseudogap

Kondo scattering processes can be divided into two classes

- H_{ch1}, H_{ch2}: **Within** the green/pink regions
- H_{1-2}: **Connecting** the green and pink regions
- Fermi liquid: $H_{ch1} = H_{ch2} \simeq H_{1-2}$

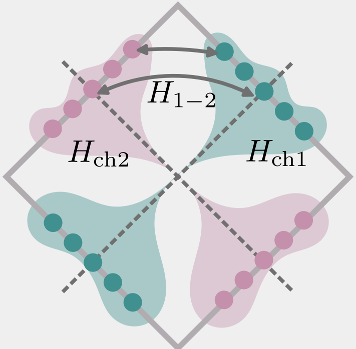

- Pseudogap: H_{1-2} **irrelevant**:

$$H = H_{ch1} + H_{ch2}$$

- Effective **two-channel Kondo** description - each pair of opposite quadrants forms a channel

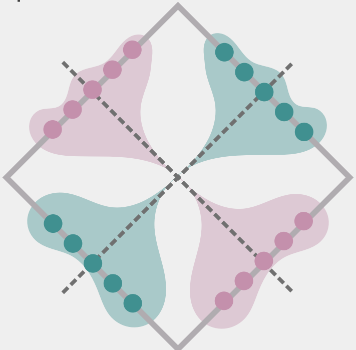

NON-FERMI LIQUID NATURE OF THE PSEUDOGAP

Non-Fermi liquid excitations of the 2CK

- **Marginal FL** behaviour: $\Sigma' \sim \omega \ln \omega$
- quasiparticle residue, $Z \sim 1/\ln \omega$ (vanishes logarithmically)
- Partially **unscreened** moment

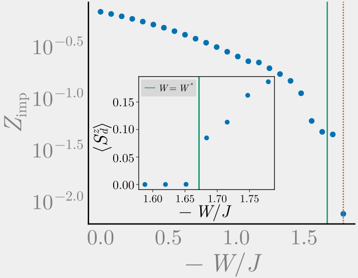

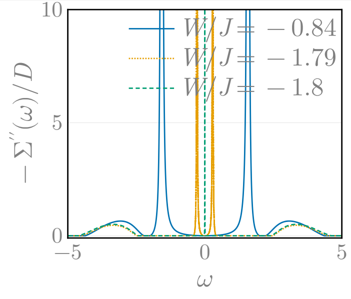

Coleman, Ioffe, and Tsvelik 1995; Schofield 1997; Varma, Nussinov, and Van Saarloos 2002; Patra et al. 2023.

Singular Nodal Metal

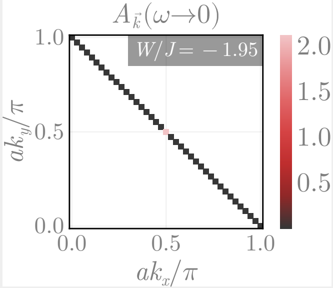

Close to the transition, Kondo cloud consists of concentrated **nodal regions**

Low-energy excitations

- Integrate out impurity spin-flips (J^2/W)
- SW transformation → effective Hamiltonian

Singular Nodal Metal

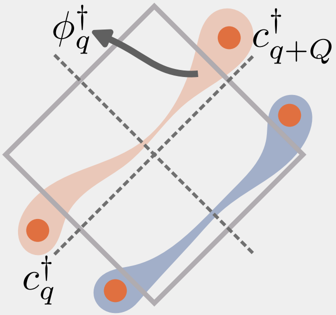

Close to the transition, Kondo cloud consists of concentrated **nodal regions**

Low-energy excitations

- Integrate out impurity spin-flips (J^2/W)
- SW transformation → effective Hamiltonian

Emergent modes: $\phi_{\mathbf{q},\sigma} = \frac{1}{\sqrt{2}}\left(c_{\mathbf{N}_1+\mathbf{q},\sigma} - c_{\mathbf{N}_1+\mathbf{Q}_1-\mathbf{q},\sigma}\right)$, $r = \phi^\dagger\phi$

Singular Nodal Metal

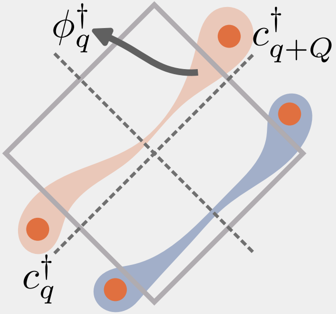

Close to the transition, Kondo cloud consists of concentrated **nodal regions**

Low-energy excitations

- Integrate out impurity spin-flips (J^2/W)
- SW transformation → effective Hamiltonian

Emergent modes: $\phi_{\mathbf{q},\sigma} = \frac{1}{\sqrt{2}}\left(c_{\mathbf{N}_1+\mathbf{q},\sigma} - c_{\mathbf{N}_1+\mathbf{Q}_1-\mathbf{q},\sigma}\right)$, $r = \phi^\dagger\phi$

$$\Delta\tilde{H} = \underbrace{\sum_{\mathbf{q},\sigma} \frac{|\varepsilon_{\mathbf{N}_1+\mathbf{q}}|\varepsilon_{\mathbf{N}_1+\mathbf{q}}}{-W} r_{\mathbf{q},\sigma}}_{\text{dispersion}} + \sum_{\mathbf{q}_1,\mathbf{q}_2,\sigma} \frac{J^{*2}}{-4W}\left[\underbrace{r_{\mathbf{q}_1\sigma}\left(1 - r_{\mathbf{q}_2\bar{\sigma}}\right)}_{\text{density interaction}} - (1-\delta_{\mathbf{q}_1,\mathbf{q}_2})\underbrace{\phi^\dagger_{\mathbf{q}_1,\bar{\sigma}}\phi^\dagger_{\mathbf{q}_1,\sigma}\phi_{\mathbf{q}_2,\sigma}\phi_{\mathbf{q}_2,\bar{\sigma}}}_{\text{fwd/tang. pair transfer}}\right]$$

Singular Nodal Metal

We focus on the simplified case of zero momentum transfer $q_1 = q_2$:

$$\Delta\tilde{H} = \sum_{\mathbf{q},\sigma} \epsilon_{\mathbf{q}} r_{\mathbf{q},\sigma} + u \sum_{\mathbf{q},\sigma} r_{\mathbf{q}\sigma} r_{\mathbf{q}\bar{\sigma}}, \quad \phi_{\mathbf{q},\sigma} = \frac{1}{\sqrt{2}}\left(c_{\mathbf{N}_1+\mathbf{q},\sigma} - c_{\mathbf{N}_1+\mathbf{Q}_1-\mathbf{q},\sigma}\right),\ r = \phi^\dagger\phi$$

$$\epsilon_{\mathbf{q}} = \frac{|\varepsilon_{\mathbf{N}_1+\mathbf{q}}|\varepsilon_{\mathbf{N}_1+\mathbf{q}}}{-W} + \frac{J^{*2}}{-4W},\ u = \frac{J^{*2}}{4W}$$

- Nodal metal is described by a **Hatsugai-Kohmoto model**.
- Non-Fermi liquid excitations.

$$\Sigma \sim \frac{u^2}{\omega}, Z \sim \omega^2$$

Σ pole continues into **Mott insulator**.

Baskaran 1991; Hatsugai and Kohmoto 1992; Phillips, Yeo, and Huang 2020.

Singular Nodal Metal

We focus on the simplified case of zero momentum transfer $q_1 = q_2$:

$$\Delta\tilde{H} = \sum_{\mathbf{q},\sigma} \epsilon_{\mathbf{q}} r_{\mathbf{q},\sigma} + u \sum_{\mathbf{q},\sigma} r_{\mathbf{q}\sigma} r_{\mathbf{q}\bar{\sigma}}, \quad \phi_{\mathbf{q},\sigma} = \frac{1}{\sqrt{2}}\left(c_{\mathbf{N}_1+\mathbf{q},\sigma} - c_{\mathbf{N}_1+\mathbf{Q}_1-\mathbf{q},\sigma}\right), \ r = \phi^\dagger \phi$$

$$\epsilon_{\mathbf{q}} = \frac{|\varepsilon_{\mathbf{N}_1+\mathbf{q}}|\varepsilon_{\mathbf{N}_1+\mathbf{q}}}{-W} + \frac{J^{*2}}{-4W}, \ u = \frac{J^{*2}}{4W}$$

- Nodal metal is described by a **Hatsugai-Kohmoto model**.
- Non-Fermi liquid excitations.

$$\Sigma \sim \frac{u^2}{\omega}, Z \sim \omega^2$$

Σ pole continues into **Mott insulator**.

For $q_1 \neq q_2$, we find **charge fluctuations**:

$$\phi^\dagger_{\mathbf{q}_1,\bar{\sigma}} \phi^\dagger_{\mathbf{q}_1,\sigma} \phi_{\mathbf{q}_2,\sigma} \phi_{\mathbf{q}_2,\bar{\sigma}}$$

Might become dominant upon **doping**!

Baskaran 1991; Hatsugai and Kohmoto 1992; Phillips, Yeo, and Huang 2020.

Non-local nature of the pseudogap

- real-space correlations and entanglement undergo a crossover within the pseudogap from short-ranged to **long-ranged** behaviour
- This is further evidence of the **breakdown of local Kondo screening**, and resulting Landau quasiparticle excitations
- the Mott transition observed by us for the Hubbard-Heisenberg model on the square lattice lies well beyond the paradigm of **local quantum criticality**

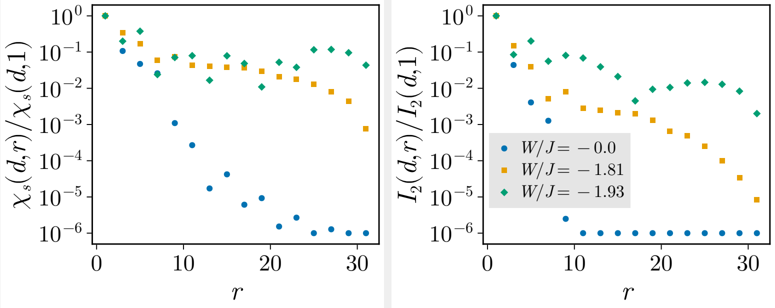

Conclusions

- On a 2D square lattice, a Fermi liquid must morph into a **non-Fermi liquid pseudogap phase** in order to give rise to a Mott insulator
- k-space differentiated **Kondo breakdown** lies at the heart of this physics
- the pseudogap features increasingly **non-local correlations** as the system is driven towards the transition

Future Directions

- Heavy fermions?
- Doping the pseudogap phase?
- Other impurity model geometries - spin liquids?

Backup Slides

Tiled Entanglement